Journal of
Synchrotron
Radiation

ISSN 0909-0495

Received 10 April 2008
Accepted 25 August 2008

Study of micro-channel geometries for internally cooled Si monochromators

P. Oberta,[a]* V. Áč,[b] J. Hrdý[a] and B. Lukáš[c]

[a]Institute of Physics, Academy of Sciences of the Czech Republic v.v.i., Na Slovance 2, 182 21, Praha 8, Czech Republic, [b]Department of Physics, Alexander Dubček University of Trenčín, Slovakia, and [c]Polovodiče a.s., Novodvorská 1768/138a, 142 21, Praha 4, Czech Republic. E-mail: oberta@fzu.cz

Rocking curves of micro-channel (MC) water-cooled monochromators are broadened by stresses introduced during fabrication and under X-ray thermal load. This is a problem which will be even more serious with the rise of the fourth-generation synchrotron sources, *i.e.* the free-electron lasers. The X-ray optics group at the Institute of Physics at the ASCR v.v.i. in Prague is designing, testing and, with company Polovodiče a.s., fabricating novel internally water-cooled Si monochromators. Here three new micro-channel geometries are introduced which reduce rocking-curve enlargement owing to the fabrication to less than 2.5 µrad (∼0.5 arcsec). All three MC designs show less rocking-curve enlargement and smoother topographic images. The designs also show better cooling efficiencies than the classical MC design in finite-element analysis calculations.

Keywords: monochromator; internal cooling; heat load.

1. Introduction

Attempts to minimize strain introduced by manufacturing and to optimize cooling efficiency of micro-channel (MC) cooled monochromators began in the 1980s. The influence of MC height and width on cooling efficiencies was studied by Oversluizen *et al.* (1989). A further study of directly water-cooled crystals for high-power insertion devices was undertaken by Oyanagi *et al.* (1995). This group studied the influence of the curvature of MCs and their distance to the diffracting surface of the monochromator. Both studies showed an improvement of the cooling efficiencies and indicated possible developments in the monochromator design. We have proposed three new MC designs and compared these with the 'classical' MC arrangement. The designs are shown schematically in Fig. 1. The overall strategy of the designs is to lower strain created due to the soldering of two Si bulks required in the MC approach. For each new MC type we have made three measurements with three different distances of the MCs to the diffracting surface. Rocking-curve measurements and topographic images are presented. The increase of cooling efficiencies is modeled by finite-element analysis (FEA) calculations.

2. Strategies to lower manufacturing stresses

We first investigated the origin of the manufacturing-induced strain in classical MC monochromators. The production of an internally water-cooled monochromator has several steps. To find exactly the point when the strain is created we recorded topographic images after the four main production steps. The first image was taken after cutting the desired shape and

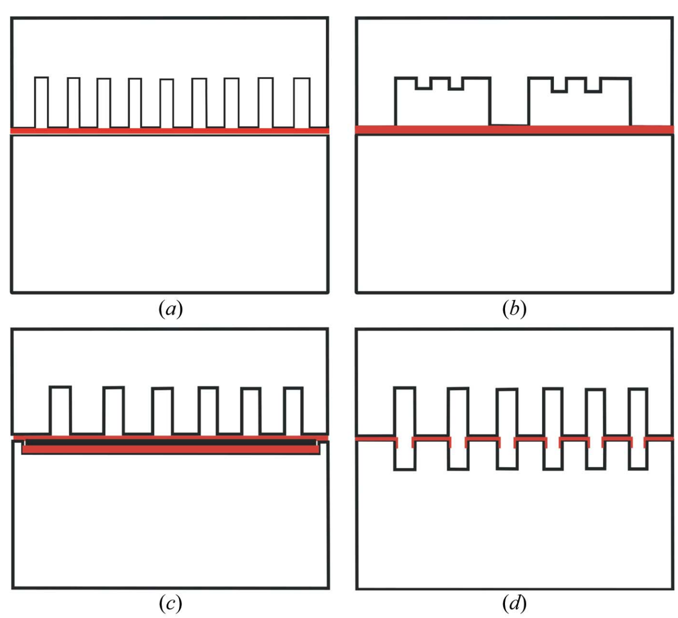

Figure 1
Proposed micro-channel geometries. (*a*) Classical design, (*b*) 2+1 design, (*c*) sandwich design, (*d*) rib-to-rib design.

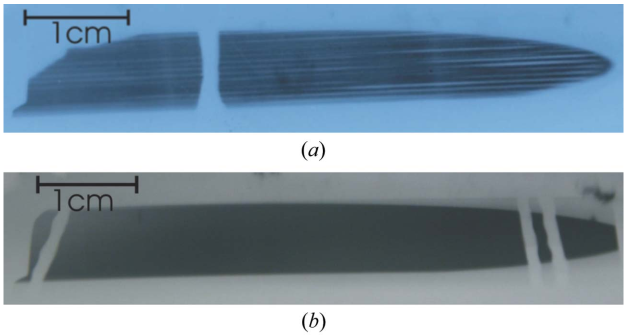

Figure 2
(*a*) Topographic image with strain map. (*b*) Topographic image without strain. The blank vertical lines in the images are due to an elastic band that fixed the sample. The left side is cut off by a slit and the curved right side is created by the arrangement of slits and the shutter of the X-ray tube. The different colors of the films are due to the use of different film companies (Kodak and Foma).

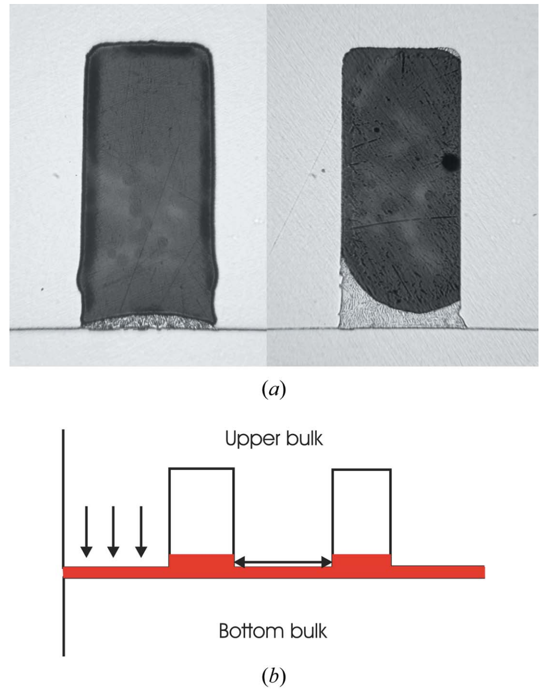

Figure 3
(*a*) The solder stays between the channel walls if MCs are etched (left). In non-etched MCs (right), the solder rises to the walls. (*b*) Places of strain creation in a MC structure, shown with arrows.

dimension of the silicon bulk, the second one after heating of this bulk to 873 K which is the soldering temperature, the third one after soldering of the two bulks together with an aluminium solder [AlSi(11,7)], and the last one after heating the soldered bulk to a temperature of 703 K in a N_2 atmosphere, which is the temperature needed to solder the water input and output pipes to the Si block. The result was obvious: the strain pattern occurred at the third step (Fig. 2). The strain is created because of the thermal expansion mismatch of silicon and the aluminium solder. Owing to this difference, stresses arise during cooling after the soldering and they are located between the bottom part of the rib and the silicon bulk. The strain pattern follows the structure of the cooling ribs. This is due to the deformations of the crystallographic planes, where the Bragg conditions are not fulfilled. White horizontal lines are clearly visible in Fig. 2(*a*), which represent the strain structure. Such structure is missing in the case without strain (Fig. 2*b*). We used Si (111) diffraction with Cu $K\alpha$ radiation. The goal of our research was to minimize this strain pattern.

One simple step to reduce the thermal mismatch strains was to etch the MCs. This process kept the solder between the ribs and prohibited a capillary attraction of the chemical solder onto the walls (Fig. 3*a*). With this approach we observed an improvement of the rocking-curve width of approximately 10% compared with non-etched MCs. For this reason we etched all MCs of the new monochromator designs. By etching the MC we suppressed one source of strain. Another source of strain arises between the MC rib and the bottom bulk (Fig. 3*b*). By choosing different MC designs we attempted to decrease the strain amount as much as possible.

To lower the strain area we first tested the '2+1' MC design (Fig. 1*b*). We compared all the results with the classical MC scheme (Fig. 1*a*), which was proposed in the 1980s and 1990s (Bilderback, 1988; Artur *et al.*, 1992). The idea of the 2+1 design is to leave out bulk-to-bulk contacts for two out of every three ribs and to enlarge the third rib, in order to provide sufficient area to tolerate high pressure (up to 5 atm) owing to the flowing water. By reducing the contact area between the two bulks, we decreased the strain surface; the area under the ribs is smaller than in the classical scheme. One advantage of this approach is that the flow space of the cooling medium between the ribs is increased which reduces the need for a high water pressure. The two small ribs between the wider bulk-to-bulk ribs reinforce the monochromator construction. The pressure due to the flow rate of the cooling medium can deform the crystal surface. In Figs. 4(*a*) and 4(*b*) we indicate the dimensions of the MCs. The thickness of the solder (red) was ~60 μm.

Second measurements were made with our sandwich design. This design consists of a classical upper diffracting bulk and a bottom support bulk. To achieve a lower strain pattern we put a 0.5 mm-thick silicon transition piece between these two bulks (Fig. 5). The function of this middle part is to compensate and absorb the stress. This stripe will adapt its shape to the different strain force of the ribs. To help support this function we used two kinds of solder. The first one, a soft solder, was used between the bottom and middle part, and the second one, a hard solder, was used between the middle and upper bulk. This way a certain amount of stress is absorbed in the stripe which is soldered together with the upper bulk to the bottom bulk with a low-temperature solder. By using a low-temperature solder we take advantage of the higher elasticity and lower strain distribution of the soldered connection.

The third MC design was the 'rib-to-rib' concept (Fig. 1*d*). One of the reasons why strain is created is the existence of solder on the walls of the ribs. Even if we etched the MCs, there remains a small remnant of solder found on the walls. The idea at the rib-to-rib design is to create a channel to

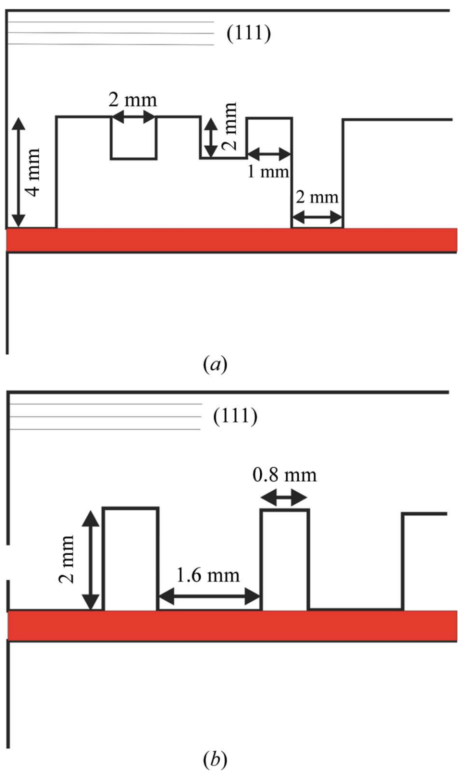

Figure 4
Dimensions of (*a*) the 2+1 MCs and (*b*) the classical MCs.

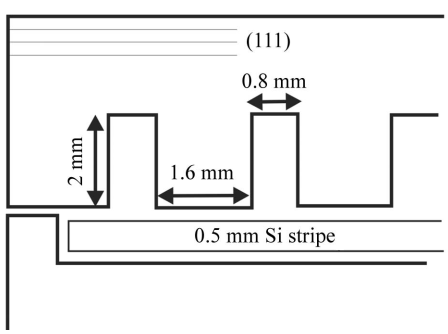

Figure 5
Scheme and dimensions of the sandwich monochromator sample. The solder is represented in red.

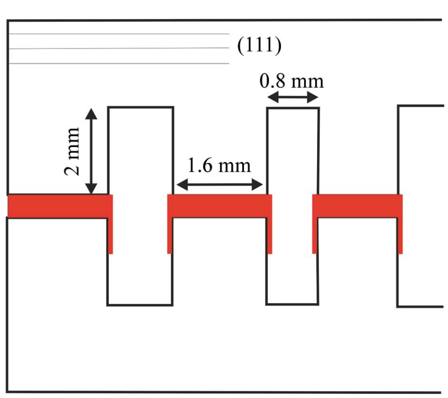

Figure 6
Scheme and dimensions of the rib-to-rib monochromator sample. The solder is represented in red.

Table 1
Measured data for the 2+1, sandwich, rib-to-rib and classical designs.

The best values are for the 2 mm layers and for the case of the rib-to-rib design, where the enlargement of the rocking-curve width is only 2.4 µrad. The featured data are an average of a series of eight measurements, with a statistical variation of maximum ±0.4 µrad. Values are for the MC orientation parallel to the impinging beam. FWHM = full width at half-maximum.

		ΔFWHM with MC parallel (µrad)			
Orientation	Thickness above MC (mm)	Classical	Sandwich	2 + 1	Rib-to-rib
(111)	2	4	3.4	2.8	2.4
	1.5	5.8	4.5	4.3	3.6
	1	7.2	6.3	5.1	4.6
(333)	2	5	3.4	1.7	0.3
	1.5	13	5.8	2.3	2.0
	1	20	7.3	2.6	2.1

accept the surplus solder and therefore eliminate a possible source of stress. Dimensions of the rib-to-rib design are shown in Fig. 6.

3. Experiment

We studied the various test designs with a double-crystal arrangement with a Seifert copper X-ray tube (Cu $K\alpha$ radiation) with a line horizontal source (Fig. 7). The measurements were performed in the (111) and (333) orientation, with MCs vertical and parallel to the impinging radiation. In all orientations we performed a series of measurements with 2 mm, 1.5 mm and 1 mm of Si over the MCs.

To measure the rocking curves we used a high-precision Huber goniometer. The topographic images were recorded both on X-ray film and with an RX4 X-ray camera (Reflex).

4. Results

4.1. Rocking-curve measurements

The rocking-curve measurements were performed for the various MCs designs. In Table 1 the differences between the measured and the theoretical values of the rocking-curve widths are presented. The table shows values for three different Si layer heights over the MCs. It can be seen that the values are better for thicker Si layers over the MCs. The presented data are only for the case when the MCs were parallel to the impinging beam. This is the orientation which is most suitable for users (Artemev *et al.*, 2001).

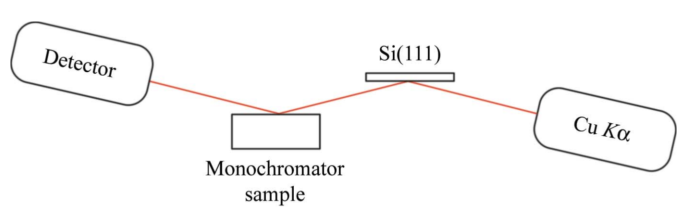

Figure 7
Experimental arrangement: detector, monochromator sample, primary Si (111) crystal and X-ray tube.

4.2. Topographic images

We have also recorded double-crystal X-ray topography images of the various monochromators. We mainly used X-ray film because of its high spatial resolution, but we also took pictures using an X-ray camera. By comparing the contrast between X-ray films for the different designs, we can observe the degree of strain; lower contrast indicates a lower strain distribution. To simplify comparison, all images were recorded under the same conditions. The X-ray tube was set to 40 kW and 20 mA and the X-ray film was exposed at a distance of 0.1 m from the sample for 5 min. This approach eliminated over-exposing. The topographic images are shown in Fig. 8. These images are for the MC orientation perpendicular to the impinging beam where the strain difference is more visible. Fig. 8(*a*) shows the case of a 1 mm layer above the MCs, and Fig. 8(*b*) shows the case of a 1.5 mm layer above the MCs. To make it more visible a gradient color map is used to indicate the strain map. Places of perfect diffraction are colored yellow. As can be seen in both cases, the rib-to-rib design corresponds to the lowest strain distribution.

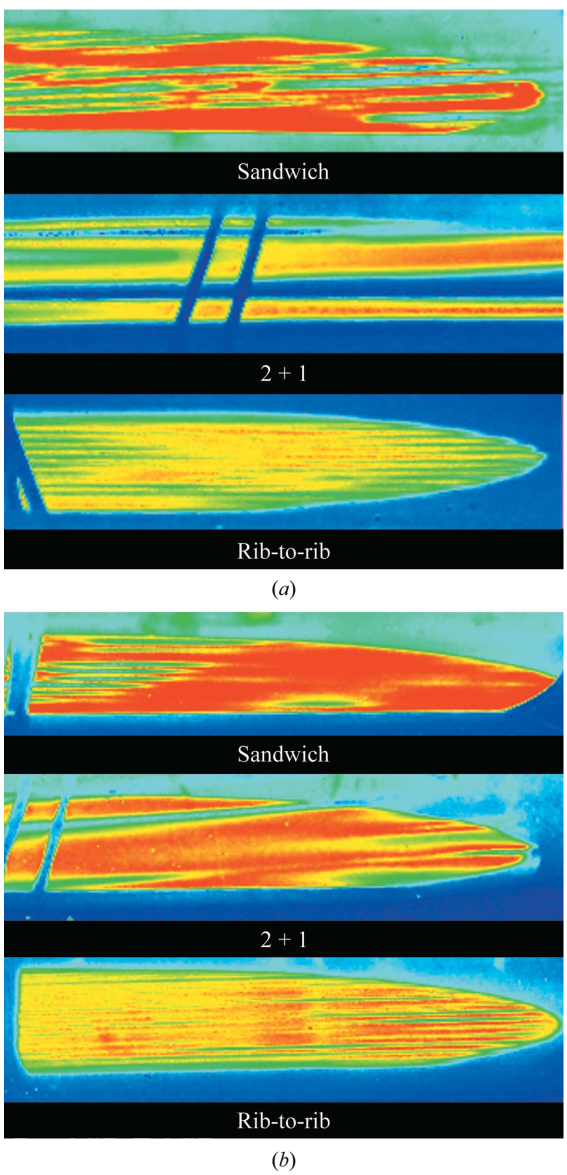

Figure 8
Topographic map in gradient false colors representing the stress distribution of different samples. (*a*) The case of a 1 mm layer above the MCs. (*b*) The case of a 1.5 mm layer above the MCs.

5. FEA calculations

To simulate high-heat-load conditions, FEA calculations were performed. As reference data we used the parameters of BM05 at the ESRF. This source is a 0.82 T bending magnet with a 24.593 m radius of curvature and a critical energy of 19.87 keV. The total power is 120 W mrad^{-1} (1.35 W mm^{-2}) and a maximum flux of 2.7 $\times$ 10^{13} photons s^{-1} mrad^{-2} (0.1% bandwidth)$^{-1}$. In all simulations the model monochromator had a Si layer thickness of 2 mm above the micro-channels. The simulations find similar surface deformations for three

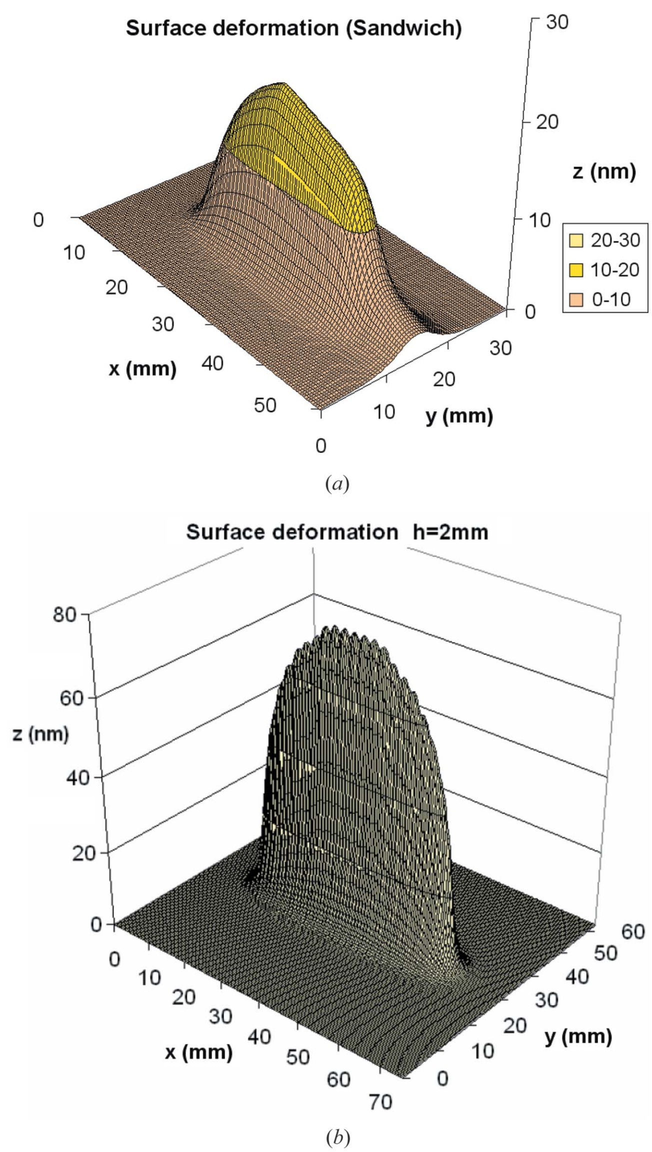

Figure 9
Surface deformations of (*a*) the sandwich design (20 nm) and (*b*) the classical design (78 nm).

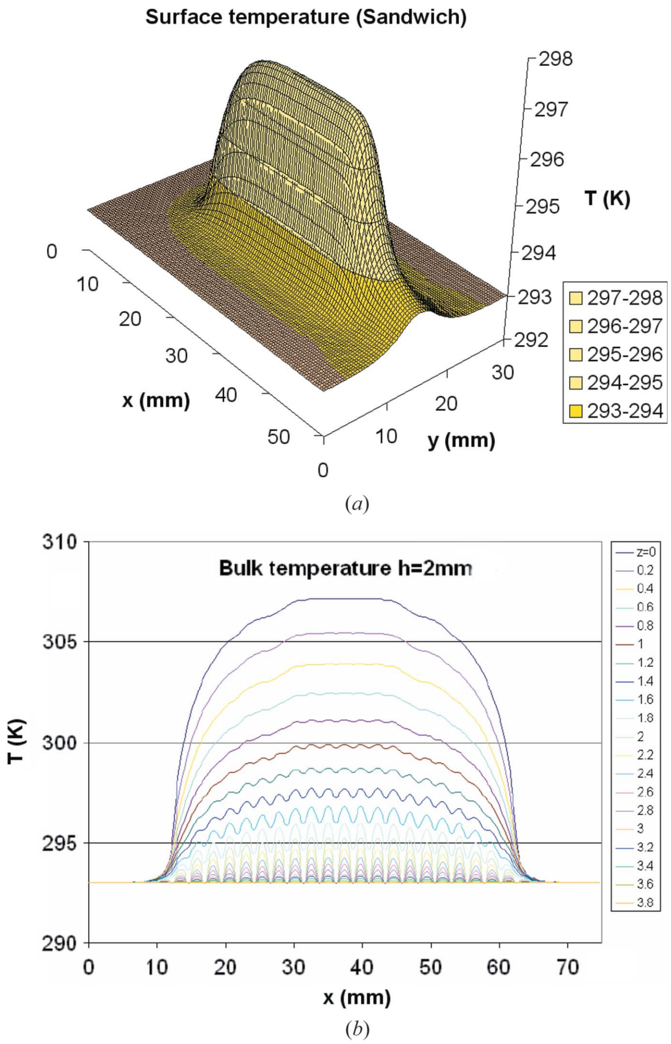

Figure 10
Surface temperature of (*a*) the sandwich design (296 K) and (*b*) the classical design (307 K).

new designs, with the best results for the sandwich design. Model surface deformations are shown in Fig. 9 for the sandwich and classical design. As can be seen, the sandwich design has a factor of two less distortion. The deformations created by the sandwich design were just 20 nm (Fig. 9*a*), followed by the rib-to-rib design with 32 nm and the 2+1 design with 35 nm. If we compare these values with the classical design (Fig. 9*b*), we find an overall improvement. The surface deformations of the classical design achieve deformations of about 78 nm.

The simulations also model the bulk temperature (Fig. 10), where z = 0 signifies the surface of the monochromator. The best result (the lowest surface temperature) is achieved by the sandwich design, with a surface temperature rise of 4 K compared with the temperature of the cooling medium. This is followed by the rib-to-rib design with a surface temperature rise of 4.2 K, then the 2+1 design with 4.5 K, with the highest surface temperature rise, 14 K, created in the classical design.

6. Results and interpretation

From the experimental rocking curves and finite-element models it is obvious that the proposed MC designs represent a significant improvement. The classical MC design had an average rocking-curve enlargement of approximately 8 µrad, using an aluminium solder and a 1 mm-thick Si layer above the MC. The rib-to-rib design pushes this value under 5 µrad and, by increasing the layer above the MCs to 2 mm, it can be lowered to less than 2.5 µrad. This, however, increases the temperature of the diffracting surface owing to a lower cooling efficiency by several K (Oberta *et al.*, 2008) at the same time it smooths the temperature variation. Most internally water-cooled monochromators are cooled using a 293 K demineralized water and this temperature can be lowered to increase the cooling efficiency and to compensate for temperature increases. By comparing the topographic images we find that the rib-to-rib design has the lowest strain distribution. It is also obvious that by increasing the thickness of the Si layer above the micro-channels we decrease the degree of deformation. From the three investigated monochromator designs the rib-to-rib design can be seen as an improvement for internally water-cooled monochromators. However, FEA calculations indicate that the lowest thermal surface deformations can be achieved with the sandwich design. Its purpose is to absorb and suppress the deformations. A theoretical model, which was used in the FEA calculation, confirmed this approach. On the other hand the topographic images showed that the highest strain and poorest image was obtained with the sandwich design. This difference between theory and experiment can be explained by the complicated manufacturing process of the sandwich design. Three pieces of silicon and two kinds of solders were used with different melting temperatures which introduce inaccuracy into the monochromator at all stages. We are confident that a more sophisticated and careful manufacturing process will allow us to achieve the theoretical values. The advantage of the rib-to-rib design is the small contact area between the upper and lower Si bulk and the absence of the side strain. This is seen in the topographic images. The results from the FEA calculations of the surface temperature are very similar. The lowest temperature was achieved by the sandwich design, followed by the rib-to-rib, and the highest temperature was achieved by the 2+1 design. If we consider all the measured and simulated data and the fabrication complexity of each design, we can say that the rib-to-rib design is a reasonable compromise. To achieve even better results we have to follow another approach than changing the micro-channel geometry. The improvement owing to the change of micro-channels has its limits. Possible ways to improve internally cooled MC monochromators is by using lower melting-temperature solders or using non-soldered designs.

This study was supported by the GAAV of the Czech Republic, contract No. IAA100100716, the Institutional Research Plan AVCR No. AVOZ10100522, and by the project

VEGA 1/4134/07 and by MVTS COST MP0601. We also thank the company Polovodiče a.s. for their crystal samples.

References

Artemev, A., Artemiev, N., Busseto, E., Hrdý, J., Mrazek, D., Plešek, I. & Savoia, A. (2001). *Nucl. Instrum. Methods Phys. Res. A*, **467–468**, 380–383.

Artur, J., Tompkins, W. H. & Trosek, C. Jr (1992). *Rev. Sci. Instrum.* **63**, 433–436.

Bilderback, D. H. (1988). *Rev. Sci. Instrum.* **60**, 1977.

Oberta, P., Áč, V. & Hrdý, J. (2008). In preparation.

Oversluizen, T., Matsushita, T., Ishikawa, T., Stefan, P. M. & Sharma, S. (1989). *Rev. Sci. Instrum.* **60**, 1493–1499.

Oyanagi, H., Kuwahara, Y. & Yamaguchi, H. (1995). *Rev. Sci. Instrum.* **66**, 4482–4486.